Ferdowsi University of Mashhad

Journal of Applied and Computational Sciences in Mechanics

Page Journal: mechanic-ferdowsi.um.ac.ir

Society of Manufacturing Engineering of Iran

Investigation of the Effect of Adding a Microtube to a Waveform Heat Sink Microchannel with Hydrophilic and Hydrophobic Surfaces for Nanofluid Flow

Akram Jahanbakhshi[1], Afshin Ahmadi Nadooshan[2], Morteza Bayareh[3]

10.22067/jacsm.2026.95513.1360

In the present work, the effect of changing the geometry of a wavy heat sink by adding a microtube and using nanoparticles to cool a CPU has been investigated. Also, the effect of sliding speed on the walls of this heat sink has been investigated based on the degree of hydrophilicity and hydrophobicity of the surfaces. In order to solve the equations, Ansys Fluent has been used, and the SIMPLE method is used for speed and pressure field coupling. Comparison of two modes with and without a microtube shows that the addition of a microtube, due to increasing the heat transfer surface and reducing the thermal resistance of remote areas of the processor, causes a more uniform distribution of CPU surface temperature. The results show that the mass flow rate of slip length with 8 µm is 45% higher than the non-slip microchannel. In a flow with a constant pressure drop, the flow velocity increases as the slip length increases. It was further found that presence of slip causes the temperature along the duct path to be at least 1 K less than non-slip mode, which means 0.3% reduction in CPU temperature.

***Keywords*: Hydrophobic surfaces, Nanofluid, Numerical simulation, Three-dimensional wavy microchannel, Wave-shaped wall.**

I. INTRODUCTION

Today, with the advancement of science and technology and the ability to manufacture cooling equipment on very small scales, there is a growing need to study the behavior of fluid flows at these scales. Therefore, in recent years, much attention has been paid to micro heat exchangers. Microsystems are used in various engineering fields such as medicine, cooling of electronic devices, transportation, aerospace, etc., and the use of microsystems is still growing rapidly. Among these, microchannels are passages with various cross-sections and microscale dimensions, which are used for transferring fluid flows and enhancing heat transfer. In other words, microchannels, due to possessing some characteristics such as large surface-to-volume ratio, high heat transfer coefficient, low required fluid volume, and small weight and dimensions, are highly practical tools. However, alongside the mentioned advantages, they also have disadvantages, including the need for complex technology for their fabrication due to their small dimensions, as well as increased pressure drop. Given the above, researchers are constantly seeking solutions to increase the efficiency of microchannels. In general, the proposed methods are divided into two categories: active and passive. In the active method, the presence of an external force is necessary to enhance heat transfer, whereas in the passive method, such a force is not required. Among the active methods, one can mention adding a magnetic or acoustic field or using vibration to create turbulence in the fluid flow and disturb the boundary layer formed on the surface. However, in the passive method, methods that do not require external force are used, such as using nanofluids, employing slip velocity and temperature jump boundary conditions, corrugating the microchannel wall, etc.

A nanofluid is a fluid to which nanoparticles have been added; hence, due to the high thermal conductivity of metal particles, the thermal characteristics of the working fluid are enhanced. In the past, these particles were on a milliscale or microscale, which, despite increasing heat transfer, caused damage to pump blades and mechanical equipment, as well as deposition in the flow path. However, today, with advancements in science and technology, particles are used

* Manuscript received July 17, 2025, Revised February 18, 2026, Accepted July 29, 2026.

[1] P.h.D, Department of Mechanical Engineering, Shahrekord University, Shahrekord, Iran,

[2] **Corresponding Author,** Professor, Department of Mechanical Engineering, Shahrekord University, Shahrekord, Iran,
Email: ahmadi@sku.ac.ir

[3] Professor, Department of Mechanical Engineering, Shahrekord University, Shahrekord, Iran.

on the nanoscale. Corrugation is also of interest due to increasing flow mixing and enhancing the heat transfer surface. Furthermore, in investigating the behavior of microsystems in engineering equipment, with a focus on enhancing heat transfer, improving the performance of microchannel heat sinks is of great interest to many engineers and researchers. The heat sink was first introduced in 1981 by Tuckerman and Pease [1], which is a thermally conductive device used for absorbing and dissipating heat from high-temperature bodies such as microelectromechanical systems.

Many researchers have investigated the thermal performance of nanofluids in microsystems assuming a slip flow regime and stated that with increasing slip coefficient, the thermal performance of the flow increases. In this regard, Duan and Muzychka [2] studied microchannels with non-circular cross-sections. They considered several common non-circular geometries for the microchannel and used the developed channel flow model to predict friction effects and Reynolds number under slip boundary conditions. In the study of Safaei et al. [3], turbulent forced convection heat transfer of water/multi-walled carbon nanotube nanofluids was studied. Turbulence was modeled using the K-ω shear stress transfer model. Simulations were performed for Reynolds numbers from 10,000 to 40,000, and nanoparticle volume fraction from 0.00% to 0.25%. Finally, an increase in the local heat transfer coefficient with increasing Reynolds number and nanoparticle volume fraction was observed for all cases. The aim of the research by Karimpour et al [4] is to study the convective heat transfer of water-copper nanofluid in a shallow inclined chamber using the lattice Boltzmann method. The upper wall of the chamber moves at a constant speed and its temperature is higher than the temperature of the lower wall. The side walls are also assumed to be adiabatic. The effects of different values of the inclination angle and volume fraction of nanoparticles have been investigated in three modes of free, forced and combined convection. The results showed that at larger values of the inclination angle and volume fraction of nanoparticles in free convection, higher Nusselt numbers can be achieved.

In an experimental study, Jung et al. [5] investigated the forced convective heat transfer of water-aluminum oxide nanofluid in microchannels and concluded that the convective coefficient of the nanofluid with a volume fraction of 1.8% nanoparticles is approximately 32% higher than the convective coefficient of pure water. Also, by reducing the dimensions of microchannels, the heat transfer coefficient at smaller Reynolds numbers equals the heat transfer coefficients in larger microchannels at higher Reynolds numbers, and in some cases is even higher, indicating the high heat transfer capability of microchannels. Ho et al. [6] studied the thermal performance of a copper microchannel with forced convection. They used water-aluminum oxide nanofluid as a coolant and ultimately concluded that using nanofluid in a microchannel heat sink significantly increases the overall heat transfer coefficient.

In a general classification, the flow regime in microchannels is determined based on the Knudsen number (which is the ratio of the mean free path to the smallest characteristic length of the body), such that if the Knudsen number is less than 0.001, the flow regime is continuous, and if it is greater than 0.001 and less than 0.1, it is a slip flow regime. Also, if it is greater than 0.1 and less than 10, the flow regime is transitional, and finally, if it is greater than 10, it is the free molecular flow regime [7]. In general, since the mean free path in liquids is much smaller than in gases (for example, for water it is about 0.17 nm), the reason for slip in fluids is not solely the molecular mean free path, but is also highly related to the surface properties of the channel and passage. According to research and studies, slip at the walls can be achieved through various methods such as chemical coatings, mechanical modifications like air grooves, or in polar fluids like water, electric and magnetic fields. Therefore, in a microchannel, the flow regime for liquids is continuous, but in some applications, the flow regime in liquids is considered to be slip, due to the use of hydrophobic surfaces alongside a hydrophilic liquid [8-9]. In the present study, slip is also created based on the degree of hydrophilicity and hydrophobicity of the surfaces. In an experimental study, Tretheway et al. [10] investigated the flow of water through a glass microchannel whose surface was coated with a thin layer of 2.3 nm thickness of a specific chemical, creating a hydrophobic surface. They examined the velocity slip at the wall and stated that this velocity slip is approximately 10% of the maximum velocity in the microchannel.

Raisi et al. [11] studied the forced convective heat transfer of a nanofluid in laminar flow in a microchannel consisting of parallel plates. The middle region of these plates is at a constant temperature, and both sides are insulated. This study was conducted for both slip and continuous flow regimes, and subsequently, the effect of slip coefficient on the thermal performance of the microchannel was investigated. Finally, Raiesi et al. concluded that the Nusselt number increases with increasing slip coefficient, which is more noticeable at higher Reynolds numbers.

Nikkhah et al. [12] numerically investigated the flow of water-functionalized multi-walled carbon nanotube nanofluid in a two-dimensional microchannel, with slip and no-slip boundary conditions, and concluded that increasing the weight percentage of solid nanoparticles and the velocity slip coefficient increases the Nusselt number. Cercignani and Daneri [13] solved the linear Boltzmann equation assuming a small pressure gradient and isothermal conditions. They used Maxwell's scattering principle to describe the interaction between the wall and the gas.

In a study by Orazio et al. [14], forced heat transfer of water-copper nanofluid in a microchannel under steady conditions was investigated. In this geometry, one half of the channel length is subjected to a constant heat flux, and the other half is insulated. This research was also conducted using the lattice Boltzmann method with a velocity slip condition and without considering a temperature jump. They conducted this study at different Reynolds numbers and slip coefficients of 0.001, 0.01, and 0.1 for volume fractions from zero to 0.04, and concluded that at each Reynolds number, with increasing volume fraction and slip coefficient, the average Nusselt number increases, and this increase is more significant at higher Reynolds numbers.

Karimipour et al. [15] investigated heat transfer of water-copper nanofluid in a microchannel with constant temperature boundary conditions, also considering velocity slip and temperature jump conditions at the surface, and

observed that the Nusselt number increases with increasing nanoparticle volume fraction at a constant slip coefficient, and at a constant volume fraction, the Nusselt number decreases with increasing slip coefficient.

Salata et al. [16] investigated the dynamic behavior of water fluid flow in a microtube with slip boundary conditions and concluded that for water fluid in a microtube, the slip length is about 0.7 to 1 micrometer. Ko et al. [17] conducted a numerical and experimental study on the pressure drop and heat transfer in a rectangular copper microchannel. In their work, numerical simulations were performed considering simultaneous heat transfer in both fluid and solid regions. The results of this study showed that the Navier-Stokes equations are capable of analyzing fluid flow and heat transfer in a microchannel. Abbaszadeh et al. [18] also numerically studied the flow of water-copper oxide nanofluid in a two-dimensional microchannel. They investigated the effect of a magnetic field considering velocity slip and temperature jump boundary conditions at the walls. Their results showed that with increasing Knudsen number, total entropy generation decreases.

Unsteady nanofluid flow in an asymmetric microchannel was investigated by Noreen et al. [19]. In this study, they performed a numerical and two-dimensional analysis of the problem by applying zeta potential and magnetic field effects, and also considered viscous dissipation and Joule heating effects. In their research, the flow was generated by the propagation of a sinusoidal peristaltic wave along the elastic walls of the channel.

Lopez et al. [20] investigated heat transfer and entropy generation in water-alumina nanofluid flow in a microchannel with a porous medium, along with the effects of flow injection/suction, velocity slip, and thermal radiation on the walls. They found that with increasing nanoparticle volume fraction and flow injection/suction, the Nusselt number on the hot wall increases and decreases on the cold wall. Akbarinia et al. [21] also investigated forced convective heat transfer of water-alumina nanofluid in a microchannel with parallel plates, considering velocity slip and temperature jump and constant temperature of the microchannel walls, and found that with a constant Reynolds number, increasing the inlet velocity increases the Nusselt number, while changing the nanoparticle volume fraction has little effect on the Nusselt number.

Al-Rashed et al. [22] in their research investigated the use of nanofluid (water/ethylene glycol 50%)-silver synthesized by the green synthesis method. They examined the effect of adding nanofluid to the system at different Reynolds numbers in a heat sink with wavy microchannels, and also, by investigating various geometrical parameters for the microchannel, they obtained the values with the highest efficiency for the wavy shape of the channel. Ghasemi et al. [23] numerically studied the combined heat transfer for three-dimensional laminar flow of water-alumina nanofluid in a triangular microchannel heat sink. The results of this study showed that increasing the nanoparticle concentration increases heat transfer and friction coefficients while thermal resistance decreases. Goldstein and Sparrow [24] experimented on heat sink microchannels in the Reynolds number range of 1000 to 1200 and concluded that corrugating the surfaces increases heat transfer compared to channels with smooth surfaces. Su et al. [25] experimentally investigated friction and heat transfer in sinusoidal microchannels with rectangular cross-sections, which consist of ten identical wavy units with an average width of 205 micrometers, depth of 404 micrometers, wavelength of 2.5 mm, and wave amplitude of 0-259 micrometers. Each test piece is also made of copper and has 60 to 62 parallel wavy microchannels. In this study, deionized water was used as the working fluid, and the considered Reynolds numbers varied from about 300 to 800. The results of this experimental study showed that the heat transfer performance of wavy microchannels is much better than that of straight microchannels. At the same time, the pressure drop increase in wavy microchannels can be much smaller than their heat transfer enhancement.

Considering that the dimensions of microchannels make fabricating microchannels with completely smooth surfaces require advanced technology, achieving such microchannels with perfectly smooth surfaces will not be easily possible in many cases. For this reason, studying wavy microchannels can help to better understand the performance of microchannels with non-smooth surfaces. Therefore, in this research, the geometry introduced by Al-Rashed et al. [22] with optimized wavelength and wave amplitude has been used as the reference geometry, and the aim is to investigate the effect of adding microtubes on the thermal and hydrodynamic behavior of the considered heat sink. The novelty of this study is the investigation of the simultaneous effect of microtubes and microchannels in a wavy heat sink structure, and subsequently, the results of both geometries (with and without microtubes) are compared with each other. Initially, the slip condition is disregarded (hydrophilic surfaces). However, in the following, the effect of the slip condition on the walls of the micro heat sink is also investigated (hydrophobic surfaces), so that based on the obtained results, it can be stated what application and effect the use of new surface technologies and creating slip in fluids will have in this equipment.

II. PROBLEM DESCRIPTION

A. Geometry and Boundary Conditions

Fig. 1 shows the geometry studied by Al-Rashed et al. [22], and Table 1 presents the dimensions of the optimized model of this geometry. According to this research, the wavy shape and dimensions of the microchannel are fixed, and subsequently, for the present study, microtubes with the dimensions mentioned in Table 2 have been added to this geometry, and finally, the geometry shown in Fig. 2 is the subject of the present research.

Using the symmetry boundary condition, only one channel has been modeled. The modeled geometry for the two cases, without microtubes and including microtubes, is shown in Fig. 3. In modeling the heat sink without microtubes, there are two computational domains, and in the case with microtubes, there are four computational domains, one of which is the solid part of the heat sink body, where only the temperature equation is solved, and the other regions are the fluid domains, where the flow and energy equations are solved numerically.

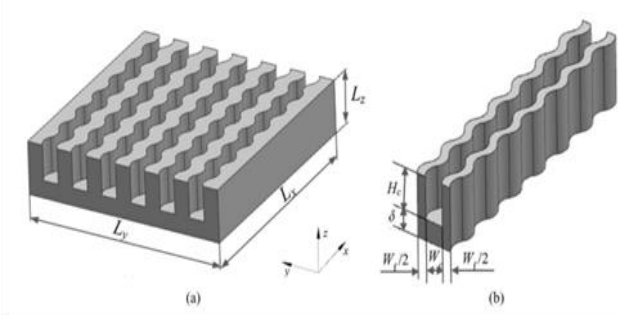


Fig. 1. Schematic of the wavy microchannel heat sink in the reference study [22]

Table 1. Geometric dimensions of the wavy microchannel heat sink in the reference study [22]

Value	Parameter
15mm	L_X
10 mm	L_Y
350μm	L_Z
120 μm	W_f
80 μm	W_C
250 μm	H_C
100 μm	δ

Table 2. Dimensional parameters of the problem geometry in the present study

Value	Parameter
10 mm	L_X
350 μm	L_Y
15 mm	L_Z
120 μm	W_f
80 μm	W_C
80 μm	D
100 μm	H_f
250 μm	H_C
200 μm	H_D

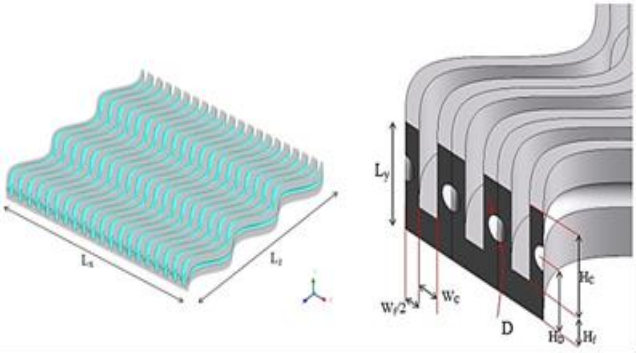


Fig. 2. Geometry of the problem.

It is assumed that the heat sink is placed on a processor (CPU), and only from its bottom surface, a heat flux of 50 W/cm² is applied to the assembly. The wavy form of the channel and tube along the geometry follows a sinusoidal function (Eq.1) [22].

$$S(z) = a_w \sin(\frac{2\pi z}{L_w}) \tag{1}$$

The values of a_w and L_w are considered based on the article by Al-Rashed et al. [22]. According to this research, $a_w = 138\mu m$ and $L_w = 5mm$ have shown the highest heat transfer and PEC among the investigated values. In the present study, this same profile has been used for the channel and tube along the length of the micro heat sink.

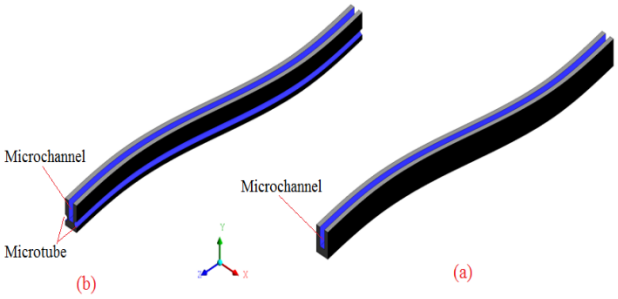


Fig. 3. Heat sink with two different geometries: (a) without microtubes, (b) with microtubes.

B. Governing Equations

In the present study, the flow is considered to be in the laminar range, and for this purpose, it is necessary to solve the conservation equations of mass, momentum, and energy for the fluid region and the energy equation for the solid region. These equations are as follows [22]:

Continuity equation:

$$\nabla.(\rho_{nf}\vec{U}) = 0 \tag{2}$$

Momentum equation:

$$\nabla.(\rho_{nf}\vec{U}\vec{U}) = -\nabla P + \nabla.(\mu_{nf}\nabla\vec{U}) \tag{3}$$

Energy equation for the fluid region:

$$\nabla.(\rho_{nf}\vec{U}C_{p,nf}T) = \nabla.(k_{nf}\nabla T) \tag{4}$$

Energy equation for the solid part:

$$\nabla.(k_S\Delta T) = 0 \tag{5}$$

In the above equations, V is the velocity vector and P is the pressure. The subscript S also refers to the properties of the solid region.

The solution method for the equations is the SIMPLE algorithm, which, by combining the continuity and momentum equations, creates an equation for solving the pressure distribution, and consequently, boundary conditions for the three components of velocity, pressure, and temperature are required to solve the problem.

Also, in this study, (water-ethylene glycol 50%) is used as the base fluid, and silver particles are used as nanoparticles. The calculations of the nanofluid mixture properties are based on the experimental research of Sarafraz and Hormozi.

Accordingly, the density, specific heat capacity, viscosity, and thermal conductivity of the nanofluid are calculated by the following equations [26]:

$$\rho_{nf} = (1-\phi)\rho_{bf} + \phi\rho_p \tag{6}$$

$$\rho_{nf} C_{p,nf} = (1-\phi)\rho_{bf} C_{p,bf} + \phi\rho_p C_{p,p} \tag{7}$$

$$\mu_{nf} = \mu_{bf}(1+2.5\phi) \tag{8}$$

$$k_{nf} = k_{bf}(0.981 + 0.00114T(c^0) + 30.661\phi) \tag{9}$$

In these equations, ρ is density, Cp is specific heat capacity, μ is viscosity, k is thermal conductivity, T is temperature, and φ is the nanoparticle volume fraction. Also, the subscript bf refers to the base fluid, p to nanoparticles, and nf to the nanofluid.

C. Parameters for Analyzing Results

By defining θ as in Equation 10, the temperature uniformity of the processor surface being cooled by the micro heat sink can be examined. Thus, the lower the value of this parameter relative to the heat flux leaving the processor, the more uniform its surface temperature.

$$\theta = \frac{T_{cpu-\max} - T_{cpu-\min}}{T_{cpu-mean}} \tag{10}$$

In this equation, the maximum temperature of the processor surface is denoted by T_{max}, its minimum by T_{min}, and the average temperature of the processor surface by T_{avg}.

The overall heat transfer coefficient of the heat sink, considering that its entire cooling performance is carried out by the convection process, is defined as follows:

$$h = \frac{q''}{T_{cpu-mean} - T_{in}} \tag{11}$$

The pumping power required for the heat sink is also calculated based on Equation (12) from the volumetric flow rate and internal pressure drop:

$$W_{pump} = \dot{V}\Delta P \tag{12}$$

D. Numerical Solution Process

To solve the equations expressed for the problem geometry, ANSYS Fluent software has been used. Also, various additional capabilities have been added to this software through coding. Furthermore, the second-order UPWIND method has been used to solve the momentum equation, and the SIMPLE method with a collocated grid has been used for coupling the velocity and pressure fields. The convergence criterion has been set to 10^{-8} for the energy equation and 10^{-6} for other equations, based on the scaled residuals.

E. Boundary Conditions

Fig. 4 shows the different numerical regions along with the eight boundary conditions used in this study, and based on the numbering, the relevant descriptions are provided.

F. Fluid-Solid Interface Wall

On these surfaces, the velocity components in the no-slip case are equal to zero, and for the case with slip condition, they have an equation dependent on the solution domain as follows. In other words, for hydrophobic surfaces, slip exists; therefore, applying the no-slip condition to model the effect of these surfaces on the flow is not possible. Thus, most numerical studies of flow adjacent to these surfaces use the Navier condition. Based on the Navier theory, the slip velocity is related to a microscopic parameter called slip length (Ls) and the velocity gradient. Ls is defined as the vertical distance from the surface at which the velocity linearly extrapolates to zero. The slip length determines the degree of surface hydrophobicity.

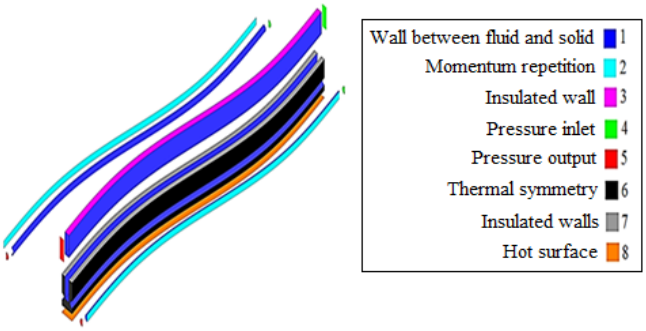


Fig. 4. Nomenclature of the boundary surfaces of the geometry.

$$\overrightarrow{U_S} = L_S \frac{\partial \overrightarrow{u_t}}{\partial \vec{n}} \tag{13}$$

On these walls, the pressure gradient normal to the plane is zero, and also, in the energy equation, the temperature and heat flux between the flow wall and the inner wall of the solid region are equal.

$$\frac{\partial \overrightarrow{p_n}}{\partial \vec{n}} = 0 \tag{14}$$

$$\left.\frac{\partial T}{\partial \vec{n}}\right|_{solid} = \left.\frac{\partial T}{\partial \vec{n}}\right|_{fluid} \qquad T|_{solid} = T|_{fluid} \tag{15}$$

G. Periodic Momentum

This surface, which is the mid-plane of the microtube, divides it into two regions due to the geometric repetition and consequently the flow repetition in the microtube. In these two regions, all velocity, pressure, and temperature parameters are equal to each other, such that these two microtube halves are connected and form a complete microtube.

H. Insulated Wall

On this wall, the velocity and pressure components are the same as the fluid-solid interface wall, and the slip condition and zero normal pressure gradient apply. However, due to the absence of a solid body above the channel, this surface is assumed to be thermally insulated, and the normal temperature gradient on it is zero

I. Pressure Inlet

These surfaces are the inlet region for the flow into the microchannel and microtube and have a constant relative static pressure, which in the present work is equal to 100 kPa. Also, the temperature is considered constant and equal to 300 K, and the velocity components are calculated based on the governing equations

J. Pressure Outlet

These surfaces are the flow outlet region and have a relative static pressure of zero (absolute pressure of one atmosphere). The velocity and temperature components in the governing equations are calculated based on the SIMPLE algorithm, the general form of which is given by Eq. (17).

$$u_{I,J,K} = u^*_{I,J,K} + d_{I,J,K}\left(p^*_{I,J.K} - p^*_{I-1,J.K}\right) \quad (16)$$

K. Thermal Symmetry

This surface is the wall of the solid region, which, based on the repeating pattern of the heat sink, separates a strip consisting of one microchannel and two half-microchannels. In this part, only the temperature equation is solved. On this surface, the gradient normal to the plane is zero.

$$\left.\frac{\partial T}{\partial \vec{n}}\right|_{solid} = 0 \quad (17)$$

L. Insulated Walls

These surfaces are the walls of the heat sink that are connected to the outside space, and in solving the energy equation, these surfaces are considered insulated

M. Hot Surface

The surface in contact with the heat source (CPU), which here is subjected to a heat flux of 50 W/cm².

III. Grid Independence Study for the Geometry without Slip Condition

A grid independence study has been performed for the geometry with the channel and tube. Table 2 summarizes this investigation. For this purpose, the Reynolds number for the channel and tube is 700 and 70, respectively, and the fluid is a 0.1% nanofluid. According to Table 3, the grid with 195,000 elements has been selected as the solution grid, and all cases have been calculated on this grid. Fig. 5 shows a view of the computational grid used.

Table 3. Results of the grid independence analysis

Mesh Number (Number of elements per thousand)	$\Delta T(K)$	$w_{pump}(W)$
24	3.386	0.0186
27	3.387	0.0475
74	3.388	0.0568
128	3.388	0.0587
195	3.388	0.0591
330	3.388	0.0591

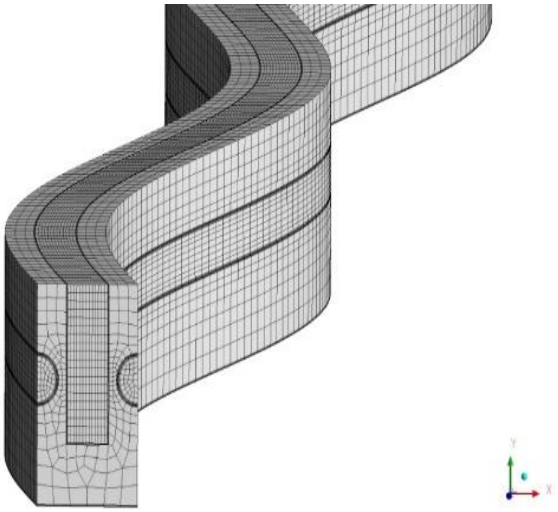


Fig. 5. A view of the computational grid used

IV. Theoretical Basis of Slip

In the present work, the first-order slip equation has been used. This equation is defined along the flow direction on the wall as follows:

$$U_s = L_s \frac{\partial U_t}{\partial n}$$
$$L_s = \alpha \dot{\gamma}^{\beta} \quad (18)$$

Due to the curvature in the wavy microchannel heat sink, the surface normal direction and the flow direction (t, n), which are shown in Fig. 6, are constantly changing, and consequently, these parameters must be calculated for each point in the numerical code. For this purpose, the following equations have been utilized:

$$\vec{U}_n = \vec{U}.\vec{n}$$
$$\vec{U}_t = \vec{U} - \vec{U}_n$$
$$\vec{t} = \frac{\vec{U}_t}{|\vec{U}_t|} \quad (19)$$

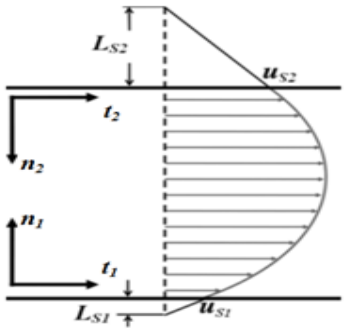


Fig. 6. Comparison of velocity profiles in slip and no-slip cases

A. Code Verification and Independence from Geometrical Angle

To verify the code's performance and its independence from

the geometrical angle (curvature of the channel surfaces), a straight rectangular channel has been examined in two different orientations: one aligned with the computational coordinate system, and the other having an angular deviation relative to the coordinate directions, as shown in Fig. 7. With identical inlet conditions, the output results should not differ between these two cases; therefore, the velocity on the wall has been compared for these two cases. The diagram in Fig. 8 shows the dimensionless slip velocity on the midline of the wall, and it is clear that using the developed code, the solution of the slip boundary condition is independent of the grid orientation in the problem geometry.

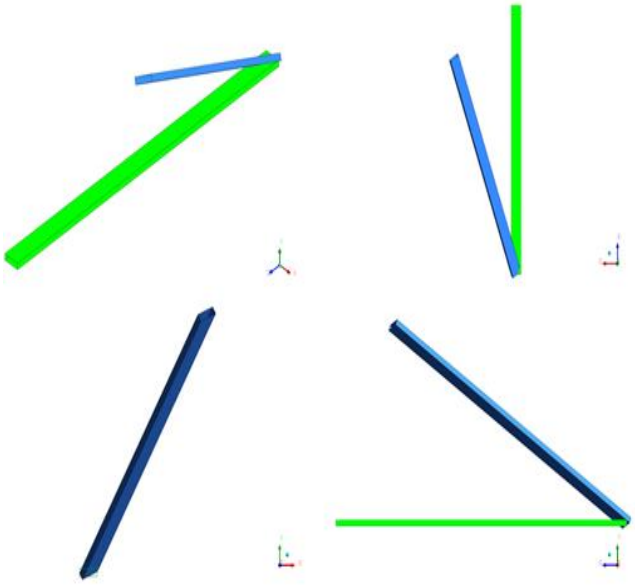


Fig. 7. Geometrical angle modeled for the channel to verify the independence of the written code from the geometrical angle

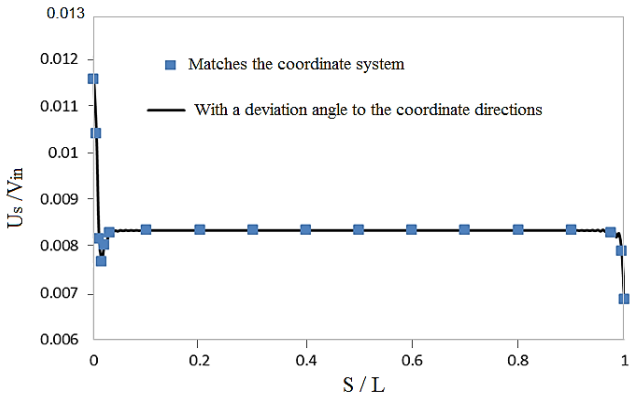
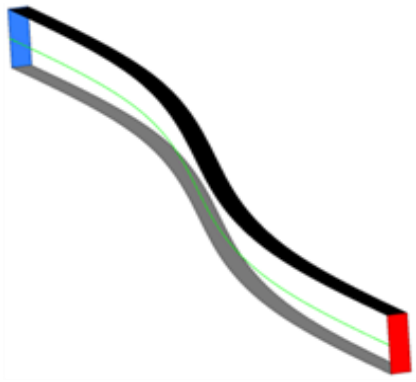


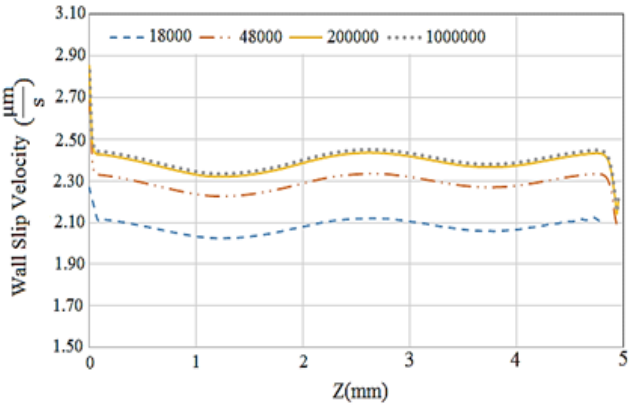
Fig. 8. Slip velocity in different directions

B. Grid Independence Study of Results with Slip

Due to the addition of the slip code to the problem (considering surfaces as hydrophobic) and solving the numerical equations on the wall, it was again necessary to investigate the effect of the grid on the solution results. Therefore, four grids with 18,000, 48,000, 200,000, and one million elements were examined, and the appropriate grid was determined. In order to evaluate the grids, the slip velocity magnitude on the midline of the wall was investigated. In Fig. 9 (a), the location of the velocity line is shown as a green curve for one wave of the channel (the studied cross-section). Based on Fig. 9 (b), the grid with 200,000 elements is suitable for modeling the flow in the desired micro heat sink with the slip boundary condition.



(a)



(b)

Fig. 9. Slip velocity magnitude on the midline of the wall for different grid refinements

V. VALIDATION OF MODELING IN SLIP AND NO-SLIP CASES

Validation of the methodology of this research has been carried out in two stages. Initially, by neglecting the slip effect, the present work was compared with the experimental results of Su et al. [25]. Based on this article, a wavy microchannel with the parameters in Table 4 was modeled. The comparison between the Nusselt number calculated by the numerical solution and the experimental results of Su et al. is shown in Fig. 10. The maximum difference between the present study and the experimental reference [25] is 8%, which corresponds to the flow at Re = 300. At Re = 500, there is a 3% error. For Re = 700, the results of the present work coincide with the experimental results of Su et al., and consequently, it is considered error-free. The results of each experiment in the study by Su et al. for each Reynolds number are shown as a range of points, which are indicated by vertical lines in Fig. 10.

Subsequently, considering the slip condition and to validate the methodology of this research, two references have been used. First, based on a constant slip length, the results were compared with the analytical solution of Ebert and Sparrow [27]. These researchers obtained an analytical solution in the form of a series for rectangular channels and presented diagrams for two different slip lengths, and

subsequently calculated the velocity profile on the wall only for a square channel. The comparison of their results with the modeling of the present work is shown in Fig. 11. Also, for a rectangular channel with a height (Hc) to width (Wc) ratio of 5, the velocity profile at the channel midline was modeled with the code of the present study and finally compared with the results of Ebert and Sparrow in Fig. 12. To verify the strain-dependent variable slip, the experimental work of Anoop and Sadr [28] was consulted, and as observed in Fig. 13, the numerical values obtained in the present article fall within the range of the experimental numbers of Anoop et al.

Table 4. Dimensional parameters of the validation problem geometry [25].

Value	Parameter
193 µm	W_f
207 µm	W_C
100 µm	H_f
406 µm	H_C
138 µm	a_W
25 mm	L_Z

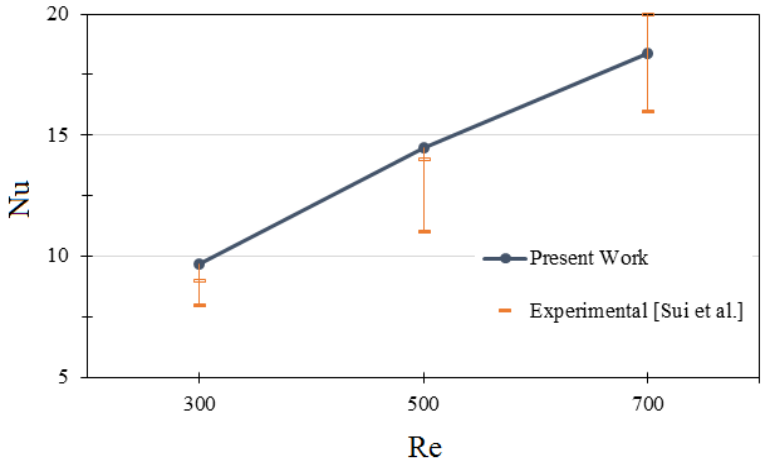


Fig. 10. Validation diagram of the present work with the research of Su et al

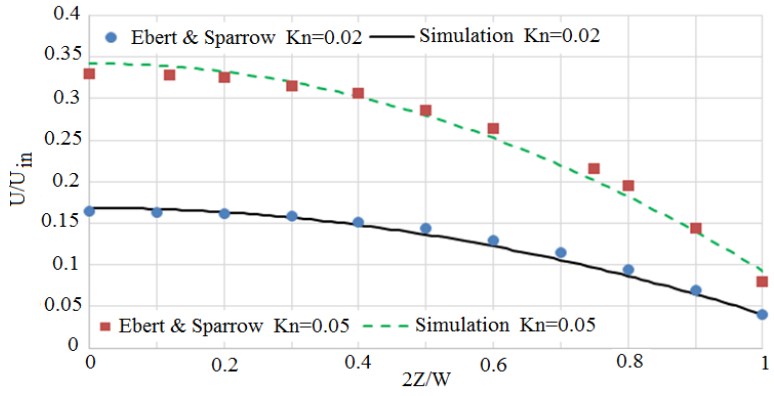


Fig. 11. Comparison of the results of Ebert and Sparrow [27] with the present work

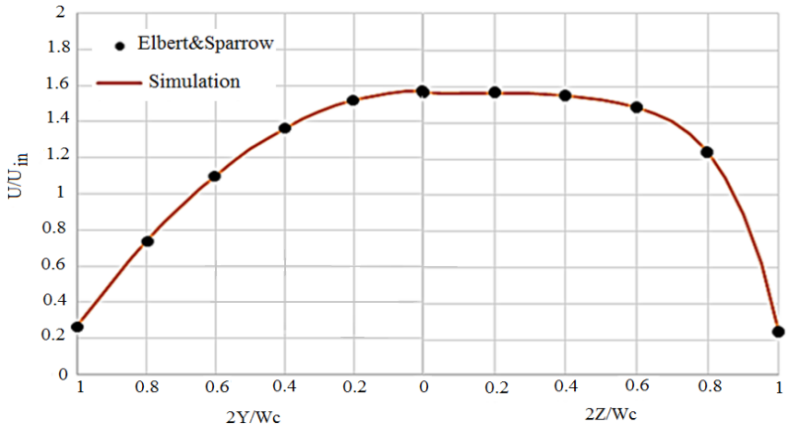


Fig. 12. Comparison of the velocity results at the midline of the rectangular channel in the present work and the results of Ebert and Sparrow [27]

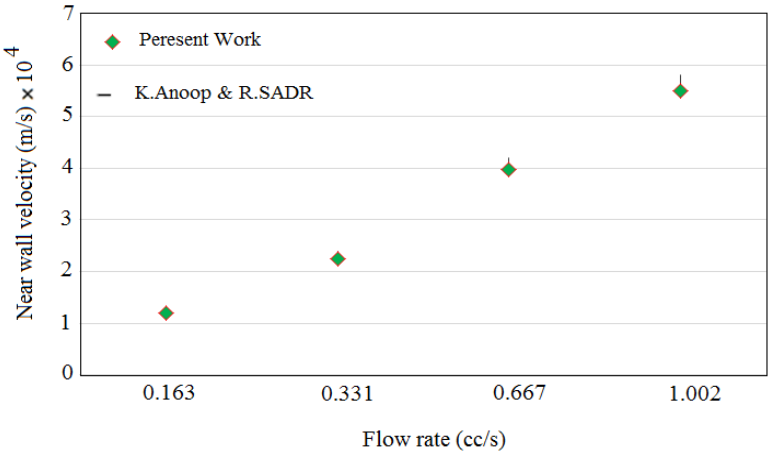


Fig. 13. Comparison of the results of Anoop and Sadr [28] with the results of the present work

VI. RESULTS

A. Effect of Adding Microtube

In the first part of this research, the effect of adding wavy microtubes on the performance of a microchannel heat sink with hydrophilic surfaces has been investigated. The modeling has been performed for silver – (water-ethylene glycol 50%) nanofluid with volume fractions of (zero, 0.1%, 0.5%, and 1%) at Reynolds numbers of (300, 500, 700, 1000, and 1500). The heat transfer coefficient for both geometries, with and without microtubes, is presented in Fig. 14. Dashed lines correspond to the case without microtubes, and solid lines correspond to the case with microtubes. This diagram shows that increasing nanoparticles and raising the nanofluid concentration in all cases increases the heat transfer coefficient. On the other hand, the higher the Reynolds number of the flow within the system, the greater the effect of increasing nanoparticle concentration.

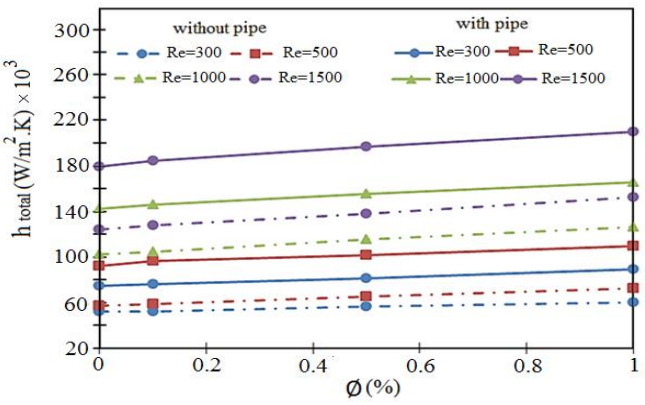


Fig. 14. Comparison of the overall heat transfer coefficient of the system in two cases: with microtube and without microtube

Comparing the two cases with and without a microtube shows that adding a microtube causes a significant increase in the overall thermal coefficient of the system. For example, the convective coefficient for flows with Reynolds numbers of 500 and 700 for the system with a microtube is respectively 80% and 110% of the convective coefficient of the system without a microtube at Re = 1000. This is because the presence of the microtube alongside the channel increases the heat exchange between the body and the fluid. On the other hand, the separation of the microchannel and tube paths and the creation of greater thermal mixing in the fluid flow cause the fluid temperature along the wall path to increase less, and the temperature difference between the fluid and the solid is maintained, which itself increases the heat transfer rate. Fig. 15 shows the ratio of temperature spread to the average temperature of the processor surface, and the smaller this number, the more uniform the temperature distribution on the processor surface. Due to the increase in the heat transfer coefficient resulting from adding nanofluid to the system, we observe improved thermal performance, and it is also observed that the temperature becomes more uniform on the surface. However, as the Reynolds number of the flow increases, due to the stronger convective term within the flow, uniformity in temperature distribution is inherently created, and consequently, the effect of adding nanofluid will not be significant. In fact, this is because with increasing Reynolds number, the flow velocity, or in other words, the mass flow rate, increases, and with increasing mass flow rate, the molecular agitation of the fluid or Brownian motion of particles increases, and as a result, the heat transfer rate increases. On the other hand, the creation of microtubes, due to increasing the heat transfer surface and reducing the thermal resistance of the distant regions of the processor, has also caused a more uniform temperature distribution on the processor surface. Fig. 16 shows the pumping power required for the flow in various investigated cases. It is quite clear that adding a microtube to the system significantly increases the total pumping power requirement of the system. For example, the pumping power for a flow at Re = 1500 without a microtube equals that for a flow at Re = 300 with a microtube. For a flow at Re = 700, approximately 6 times the pumping power is required compared to a flow at Re = 1500 without a microtube. On the other hand, this figure shows that adding nanofluid to the system reduces the required pumping power. This phenomenon occurs due to the decrease in flow velocity resulting from the increase in fluid density while maintaining the Reynolds number. In other words, in conventional energy-carrying fluids, increasing the convective heat transfer requires increasing the fluid velocity and raising the Reynolds number, and consequently the Nusselt number, and thus the convective heat transfer coefficient. This increase in velocity in equipment, in turn, requires increasing the pump

power consumption. However, if a nanofluid is used, at a given velocity, the increase in heat transfer results from the increase in the fluid's thermal conductivity. For example, increasing heat transfer by a factor of 2 using a base fluid requires increasing the pump power by about 10 times. Whereas if nanoparticles are added to the base fluid and the thermal conductivity of the resulting nanofluid becomes about 3 times that of the base fluid, the same twofold increase in heat transfer can be achieved without needing to increase pumping power. Therefore, reducing energy costs and reducing pump power consumption are among the advantages of using nanofluids in micro heat sinks.

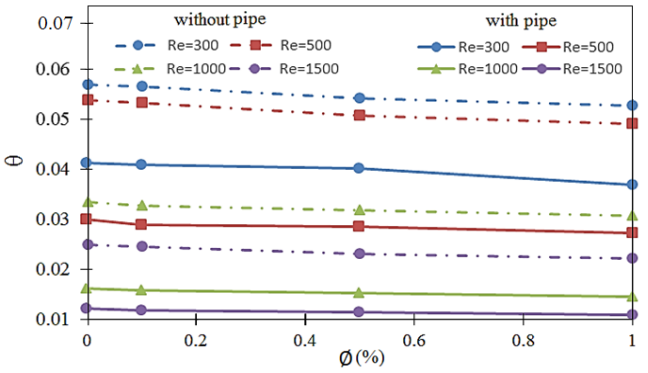


Fig. 15. Investigating temperature uniformity with Θ

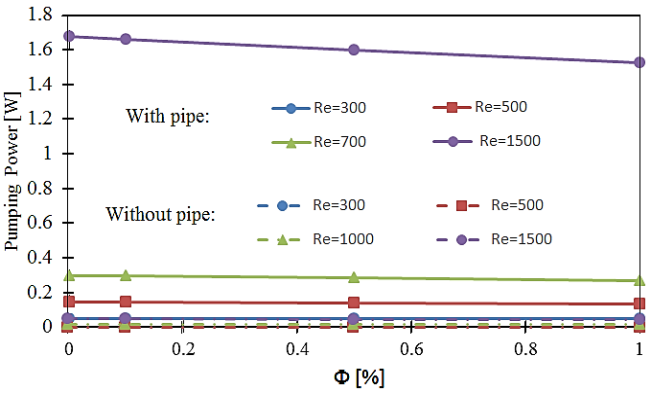


Fig. 16. Pumping power at different Reynolds numbers and concentrations

The more uniform the temperature inside the channels, the better the flow mixing and the more appropriate the performance of that thermal channel. Figs. 17 and 18 show the temperature contours of the nanofluid in the wavy outlet region of the microchannel and tube. To properly display the desired information, the image related to the microtube has been magnified non-uniformly, only in the transverse direction, so that a full arc (at the outlet) of the microtube can be observed. In Fig. 17, for all cases, the flow wall is hotter than its central part, but in Figures (a) and (b), the temperature of the central part remains unchanged, and the effect of increasing nanoparticles in heat diffusion from the walls to the center of the flow is not distinguishable.

This result is due to the high flow velocity and the stronger convective power of the flow in its streamwise direction compared to the conductive heat diffusion power in the direction perpendicular to the flow. Thermal mixing in the fluid flow means better heat transfer to the central part of the flow in the microtube or microchannel. In this section, due to the no-slip law at the walls and the establishment of the laws of conservation of mass and momentum, the fluid flow is more intense in its central part, and consequently, the passage of more fluid mass causes a greater concentration of thermal capacity in the central part of the flow. Now, the better the fluid mixing, the better and faster the heat near the walls is transferred to the center of the flow, which will reduce the temperature gradient required to transfer a certain amount of heat from the wall to the center of the flow. In the present work, two factors lead to the improvement of this mixing. The first factor is the curvature in the geometry of the channel and microtube, and the other factor is adding nanoparticles to the fluid and increasing the thermal conductivity coefficient of the fluid, and in fact increasing the Prandtl number of the fluid flow. In Figures (c), (d), and (e), which correspond to Re = 300, due to the lower convective power of the flow, the heat diffusion in the direction perpendicular to the flow has occurred better, and the increase in nanoparticles has accelerated this phenomenon, such that temperature changes have also reached the center of the flow. For the temperature to reach the central core of the flow, a temperature gradient in the direction perpendicular to the flow path is needed, and this means an increase in the fluid temperature at the wall.

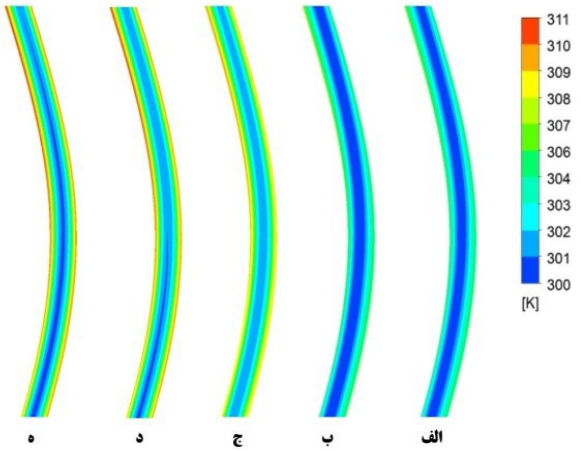


Fig. 17. Temperature distribution in the rectangular channel: a) Re=700, φ=1% b) Re=700, φ=0.1% c) Re=300, φ=1% d) Re=300, φ=0.5% e) Re=300, φ=0.1%

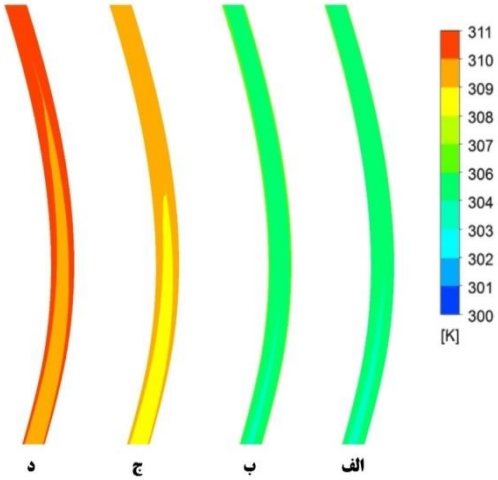


Fig. 18. Temperature distribution in the microtube: a) Re=700, φ=1% b) Re=700, φ=0.1% c) Re=300, φ=1% d) Re=300, φ=0.1%.

In the contours of Fig. 18, similar to the discussion for the rectangular channel, the same trend applies to the microtube. Due to the smaller cross-section, the heat transfer flow in the vertical direction has acted much more strongly, and as a result, greater temperature changes are observed. Also, Figs. 17 and 18 show that the effect of adding nanoparticles on the performance of the microchannel and microtube is positive, but its positive effect decreases with increasing Reynolds number of the flow.

C. Effect of Velocity Slip at the Walls

In the following, the effect of velocity slip at the walls (hydrophobicity of surfaces) on the performance of the heat sink is investigated. By considering the fluid properties independently of temperature due to the low temperature variations, the velocity distribution results are independent of the energy equation and temperature. Therefore, first, the results of velocity distribution and the effect of slip on pure fluid flow are presented

D. Velocity Distribution in the Microchannel

Fig. 19 shows the flow velocity magnitude at the midline of the microchannel for the no-slip case and two slip lengths of 4 and 8 micrometers. Considering the constant pressure drop (equal to 100 kPa) in the microchannel, with increasing slip length, the friction effect at the flow wall has decreased, and consequently, the flow encounters less resistance. It is clear that in a flow with constant pressure drop, with increasing slip length, the flow velocity increases.

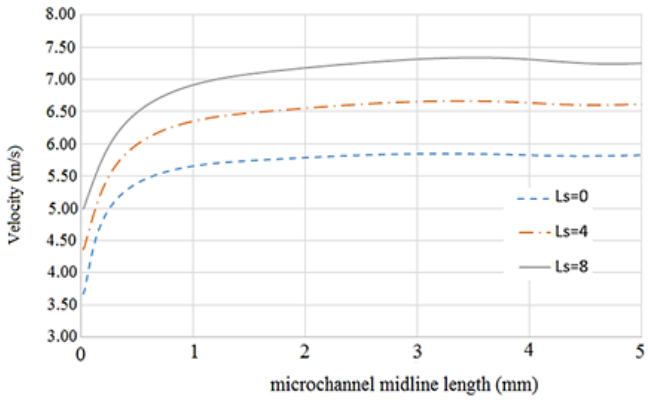


Fig. 19. Velocity magnitude at the midline of the microchannel.

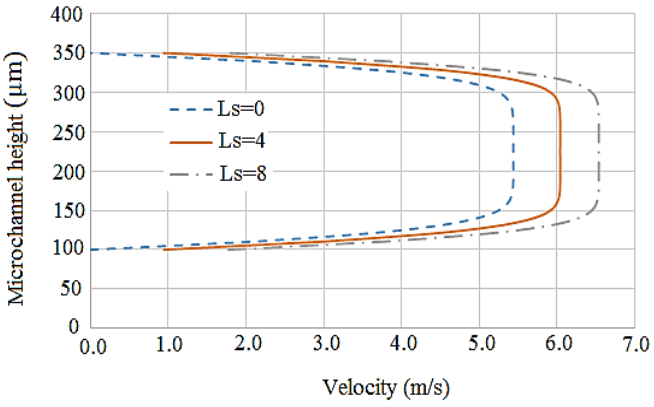
In Table 5, the velocity value at the midline of the microchannel and its mass flow rate at a pressure drop of 100 kPa are presented, and it is clear that the mass flow rate of the flow with a slip length of 8 micrometers is 45% higher than that of the microchannel without slip at the walls.

Table 5. Comparison of the effect of wall slip length on velocity components in the microchannel

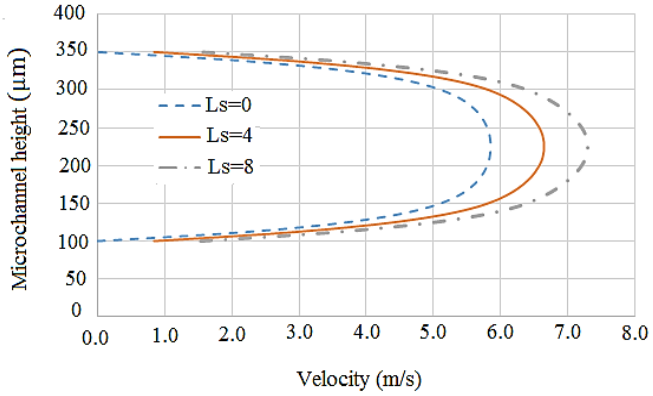
Slip length (μm)	Average velocity in the middle of the microchannel (m/s)	Microchannel mass flow rate (mg/s)
0	5.685	70.050
4	6.434	86.875
8	7.050	101.195

Fig. 20 shows the velocity profile at two distances from the inlet, where graph (a) is in the developing region and graph (b) is in the fully developed region of the flow. Due to the rectangular cross-section of the channel as well as its sinusoidal curvature, the slip velocity is not uniform at all points on the wall. With increasing slip coefficient, the slip velocity magnitude increases, and for both slip lengths of 4 and 8 (micrometers), with increasing distance from the microchannel inlet to the start of the fully developed region, the slip velocity has a decreasing trend, and after this region, it reaches a constant value.

The reason for this is the decrease in velocity gradient from the inlet to the fully developed region. Also, comparing the two graphs (a) and (b) shows that the velocity slip in the developing region is greater due to the steeper velocity gradient. To better observe this point, Fig. 21 is presented, which shows the flow velocity on the wall for two slip lengths of 4 and 8 micrometers. In this figure, apart from the obvious effect of increasing slip velocity with increasing slip length, it is observed that in the corners, the velocity is lower, and also the velocity on the side walls (wider surfaces) is higher because there is less obstruction against the flow.



(a)



(b)

Fig. 20. Heat sink geometry with and without microtube: a) Velocity profile in the developing region (at a distance of 0.5 mm from the inlet), b) Velocity profile in the fully developed region (at a distance of 4.5 mm from the inlet).

The effect of channel curvature on the wall velocity is also evident, such that as the wall turns towards the flow, the velocity on the wall increases, and as the wall turns opposite to the flow, the velocity on the wall decreases. The slip

velocity depends on the velocity gradient near the wall, and in fact, the larger the slip length, the better the fluid molecules can escape in regions with higher shear stress, and consequently, they acquire higher velocity on the wall. This reasoning is more evident in Fig. 22, which shows a three-dimensional representation of the velocity profile in the cross-section.

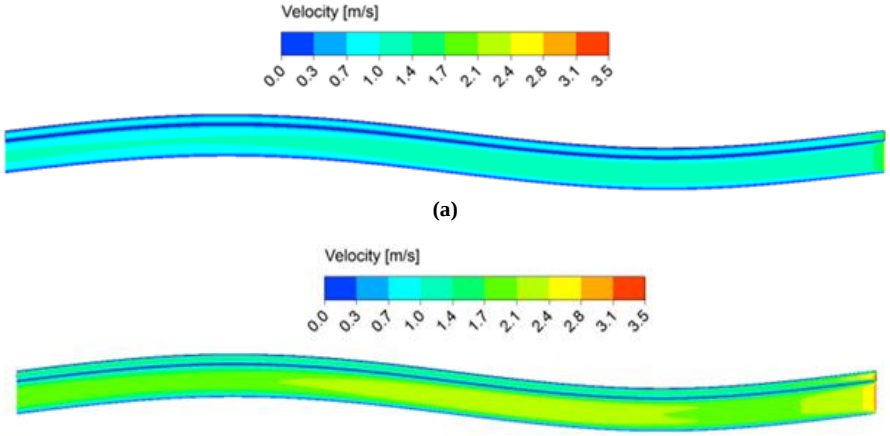


Fig. 21. Velocity on the microchannel wall: a) 4-micrometer slip, b) 8-micrometer slip.

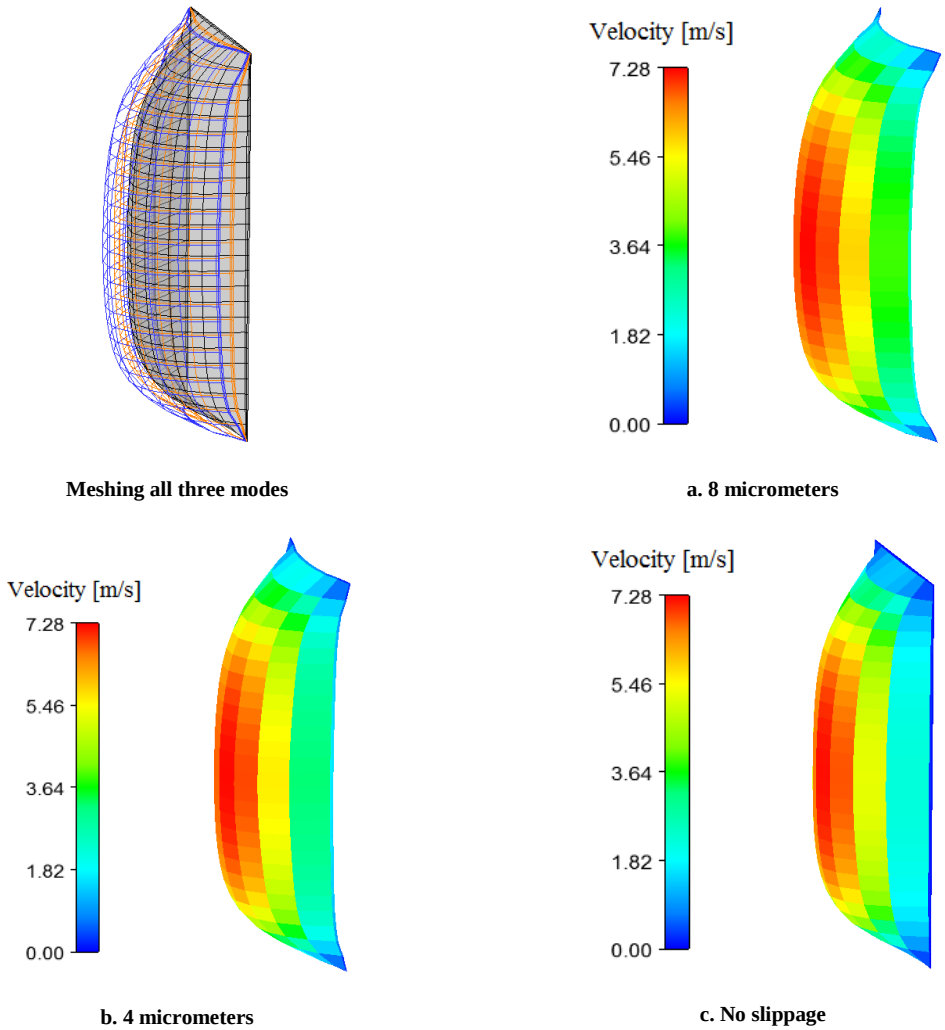


Fig. 22. Velocity profile at 4.5 mm from the flow inlet.

E. Temperature Distribution in the Microchannel

Given the flow behavior investigated in the previous section, it is obvious that due to the increased flow in the microchannel, we expect more favorable performance from the channel with a larger slip length. The following results also demonstrate this point. Fig. 23 shows the temperature diagram on the hot surface along the path.

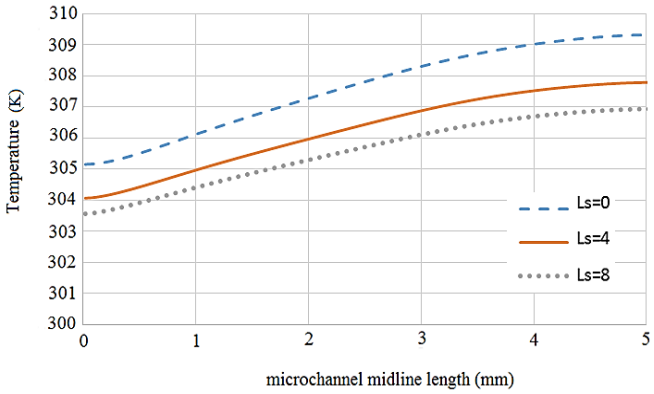


Fig. 23. Temperature of the hot surface of the heat sink along the path.

As observed in Fig. 23, the presence of slip (hydrophobic surfaces) has caused the temperature along the path to be at least one degree Kelvin lower than the no-slip case, which means a 0.3% reduction in surface temperature. It should be noted that this performance is passive, and in fact, the pumping cost of the flow has remained constant. Therefore, regardless of the economic aspects of producing these surfaces, their use reduces the required pumping power and not only does not decrease the heat transfer efficiency of the system but actually increases it to some extent. Fig. 24 shows the temperature diagram at the midline of the microchannel at a distance of 4.5 mm from the inlet. This diagram shows that the energy absorbed by the fluid has not penetrated to the center of the flow and has only increased the temperature in a 50-microliter layer. In the no-slip flow, the fluid temperature at the wall has increased by a maximum of 10 degrees.

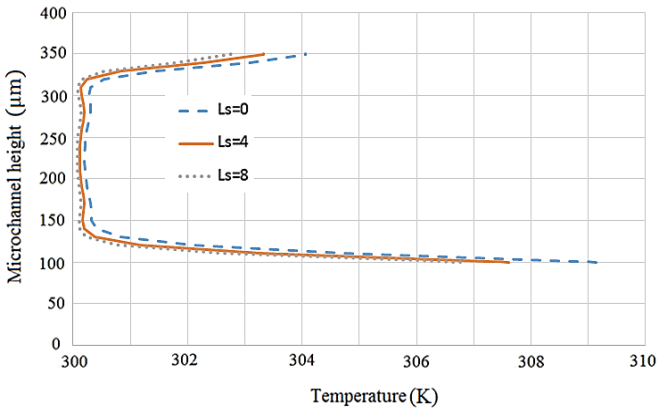
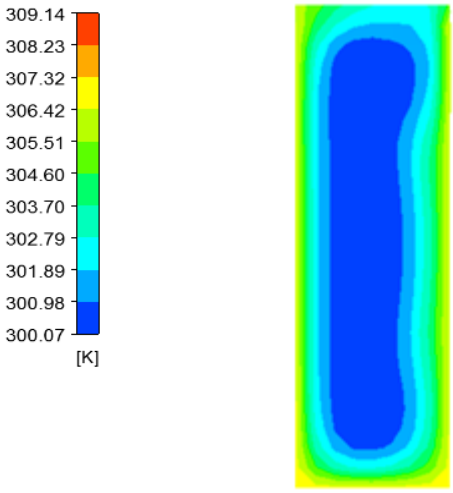
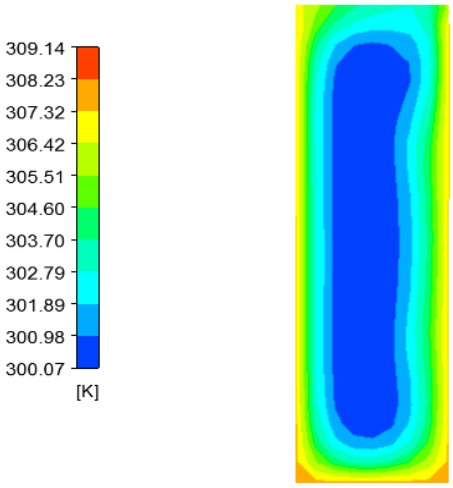


Fig. 24. Temperature diagram at a distance of 4.5 mm from the flow inlet.

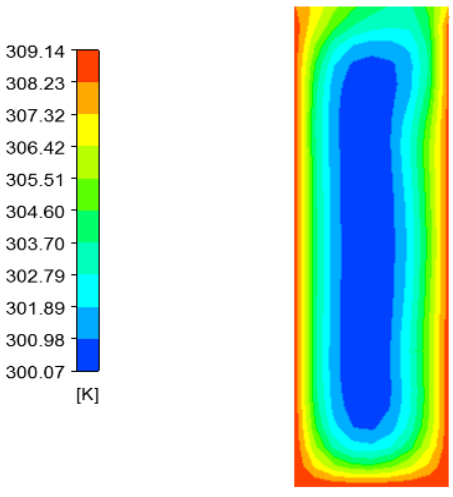
Fig. 25 also shows the temperature distribution in the channel cross-section, and as stated, the thermal energy absorbed by the fluid has not reached its central core. Another point is that the largest volume of hot fluid is at the bottom of the channel, which is closest to the heat source. Consequently, it seems that for using a microchannel, the closer its location is to the bottom of the heat sink, the better the effect.



a. 8 micrometers



b. 4 micrometers



c. No slippage

Fig. 25. Temperature profile in the outlet cross-section of the microchannel.

F. Velocity Distribution in the Microtube

Fig. 26 shows that in the microtube as well, with increasing wall slip velocity, which reduces wall shear stress, at a constant pressure drop, the flow rate increases and the velocity becomes higher. In the two cases shown, the mass flow rates are 8.09 and 10.39 mg/s, respectively. Another point is the difference in slip velocity at different parts of the wall, which is caused by its sinusoidal form. Fig. 27 shows the slip velocity diagram on the bottom side and also on the right side of the microtube wall, for a slip length of 2 micrometers. Due to the wall curvature and geometrical changes that cause pressure variations in the flow, velocity changes for the side part of the wall are evident. Also, the wall in the slip condition has a limited ability to apply shear stress in the flow direction, which causes changes in the velocity on the wall.

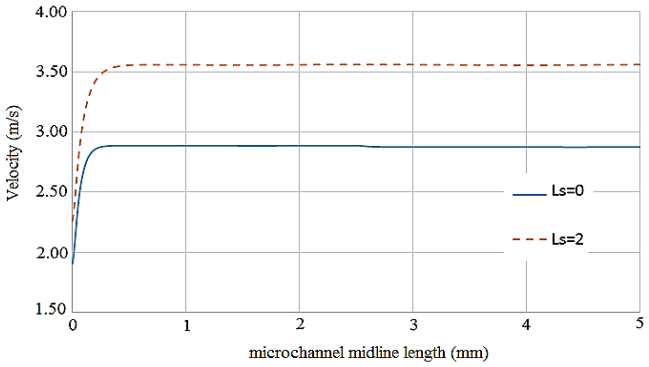


Fig. 26. Comparison of velocity distribution at the midline of the microtube for zero slip and a slip length of 2 micrometers

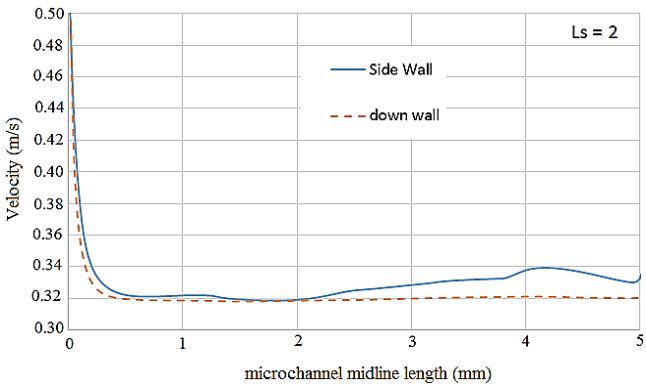


Fig. 27. Slip velocity on the bottom and side surfaces of the microtube

G. Investigation of Heat Transfer in the Microtube

Fig. 28 shows that adding a microtube to the heat sink causes the temperature on the hot surface to decrease by more than one degree. However, creating a slip of 4 micrometers on the channel wall has also shown similar performance and has caused a one-degree reduction in the hot surface temperature. By adding a microtube to the channeled heat sink with a slip condition, it has been observed that the hot surface temperature has again decreased by more than one degree. For example, at a distance of 1 mm, for the combined geometry (including microtube and microchannel) and a slip length of 4 micrometers, the temperature on the hot surface is about 303.9 K, while for the geometry including the microchannel with the same slip length and the combined geometry without slip, the temperatures are close to 304.97 K and 304.99 K, respectively. This value for the geometry with the microchannel without considering slip is approximately 305.11 K. At a distance of 5 mm, these temperatures are approximately 306.44 K, 307.86 K, 304.89 K, and 309.35 K, respectively.

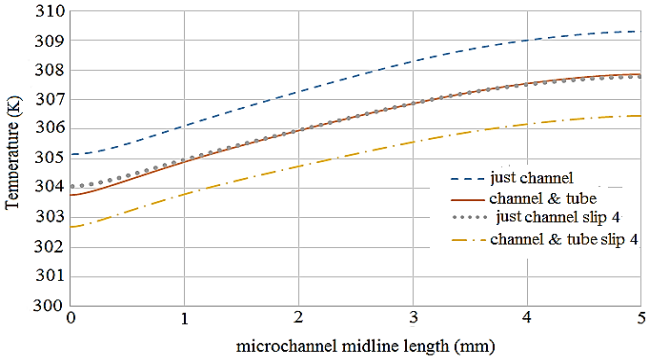


Fig. 28. Comparison of hot surface temperature with and without microtube

VII. Investigation of the Effect of 1% Silver Oxide Nanofluid in Water-Ethylene Glycol 50% Base Fluid

In this stage, the flow in the microchannel heat sink without a microtube has been modeled in two cases: no-slip and with a slip length of 8 micrometers, using water-ethylene glycol 50% base fluid and nanoparticles with a volume fraction of 1%. Subsequently, temperature changes along the hot surface and the center of the microchannel, mass flow rate, and velocity profile at the centerline of the microchannel have been investigated. The modeling has been performed with a constant pressure drop of 100 kPa over a length of 5 mm. In this stage, it has been assumed that the presence of nanoparticles does not disturb the performance of the slip walls, and the slip length of the nanofluid is the same as that of the base fluid in an identical channel, because it is considered that this slip is based on changes in the physical and chemical properties of the surface and consequently has no effect on the characteristics of the working fluid, and does not cast doubt on its single-phase assumption.

A. Hot Surface Temperature

In the diagram of Fig. 29, it is observed that using nanofluid reduces the hot surface temperature, but the effect of using 1% nanofluid (which is the highest volume fraction studied in this work) is less than the effect of creating 8-micrometer slip (which is the highest slip length studied). For example, at a length of 1 mm, for the base fluid without slip condition, the temperature is about 306 K, and for the nanofluid under the same conditions, it is approximately 305 K. Considering an 8-micrometer slip length, these temperatures are about 304.5 K and 303.7 K, respectively. In fact, using nanofluid in a slip microchannel somehow combines their effects and is better than the two single-effect cases, i.e., adding nanofluid without slip or using pure fluid with slip. In this diagram, Ls refers to the slip length, and BF and Nano refer to the base fluid and 1% nanofluid, respectively.

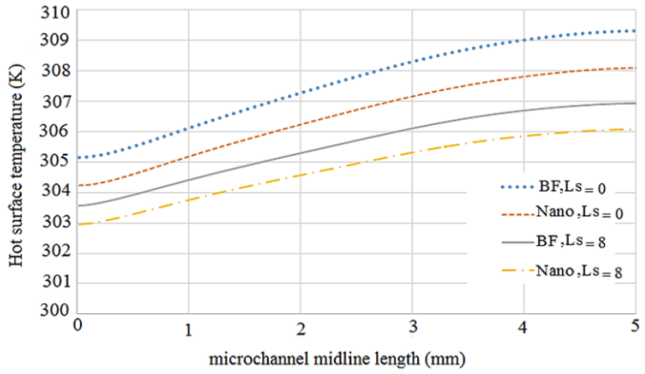


Fig. 29. Investigation of temperature along the hot surface of the micro heat sink

B. Velocity Profile in the Center Plane of the Outlet

The diagram in Fig. 30 shows that at constant pressure drop, increasing nanoparticles reduces the peak of the velocity profile, which is due to the decrease in flow rate resulting from the increase in fluid viscosity and density. However, it should be noted that no significant effect on the slip velocity magnitude is observed. Table 6 shows that using nanofluid increases the mass flow rate, but due to the increase in density, the flow velocity has decreased.

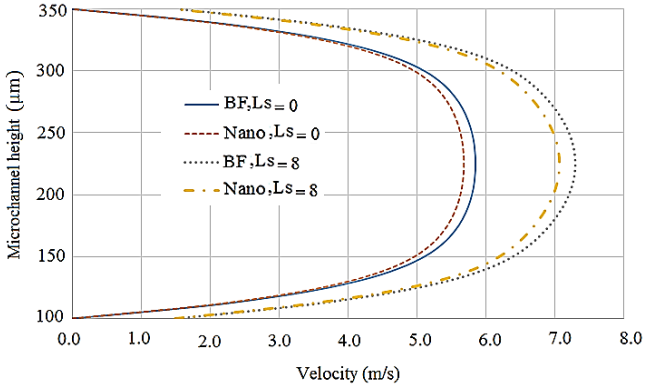


Fig. 30. Velocity profile at the centerline of the outlet plane.

Table 6. Mass flow rate in different cases

Mass Flow Rate (mg/s)	(Slip length μm)	Fluid
70.05	0	Base fluid
74.07	0	Nanofluid 1%
101.20	8	Base fluid
106.79	8	Nanofluid 1%

C. Temperature at the Centerline of the Microchannel

The diagram in Fig. 31 shows very slight changes (on the order of 0.1 K) for the different cases, but the concept it conveys is that using nanofluid has caused the temperature to increase more significantly at the center of the microchannel. Given that adding nanoparticles to the base fluid increases density and thermal conductivity while decreasing specific heat capacity, ultimately, the increase in thermal conductivity has been more dominant, leading to better heat transfer and more heat being transferred to the core of the flow.

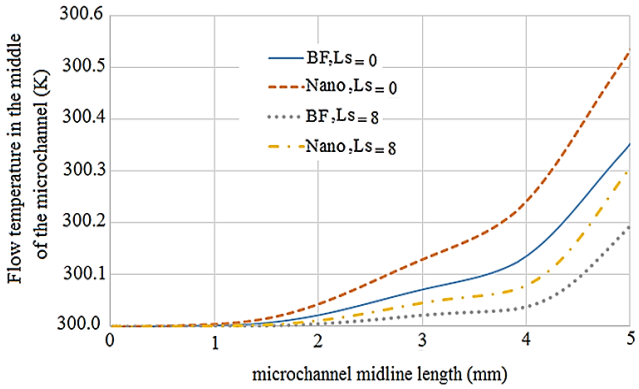


Fig. 31. Temperature at the centerline of the microchannel

VIII. CONCLUSIONS

In thermal systems, the heat transfer coefficient increases by changing the flow geometry, boundary conditions, or by improving the thermophysical properties of the fluid and the heat exchanger material. In this paper, the thermal and hydrodynamic behavior of a wavy microchannel heat sink, with and without the presence of microtubes, for pure fluid and nanofluid (water-ethylene glycol 50%), has been compared. Additionally, the effect of velocity slip based on the hydrophobicity of the walls of this micro heat sink was investigated and compared with the no-slip case. Comparing the two cases with and without a microtube shows that adding a microtube causes a significant increase in the overall thermal coefficient of the system. For instance, the convective coefficient for a flow at Re = 500 for the system with a microtube is 80% of the convective coefficient of the system without a microtube at Re = 1000. This is because the presence of the microtube alongside the channel increases heat exchange between the body and the fluid. On the other hand, the separation of the microchannel and tube paths and the creation of greater thermal mixing in the fluid flow cause the fluid temperature along the wall path to increase less, maintaining the temperature difference between the fluid and the solid, which itself increases the heat transfer rate. Furthermore, the addition of microtubes, due to increasing the heat transfer surface and reducing the thermal resistance of the distant regions of the processor, has also resulted in a more uniform temperature distribution on the processor surface. It was also concluded that under constant pressure drop conditions in the microchannel, increasing the slip length reduces the friction effect at the flow wall, and consequently, the flow encounters less resistance. It was found that in a flow with constant pressure drop, increasing the slip length increases the flow velocity. On the other hand, due to the rectangular form of the channel and its sinusoidal curvature, the slip velocity is not uniform at all points on the wall. It was also observed that using nanofluid reduces the hot surface temperature; however, the effect of using nanofluid with a concentration of 1% is less than the effect of creating slip. Nevertheless, using nanofluid in a slip microchannel effectively combines their effects and performs better than either single-effect case individually.

REFERENCES

[1] D. B. Tuckerman and R. F. W. Pease, "High-performance heat sinking for VLSI," *IEEE Electron*

Device Letters, vol. 2, no. 5, pp. 126–129, 1981. [Online]. Available: https://doi.org/10.1109/EDL.1981.25367

[2] Z. Duan and Y. S. Muzychka, "Slip flow in non-circular microchannels," *Microfluidics and Nanofluidics*, vol. 3, no. 4, pp. 473–484, 2007. [Online]. Available: https://doi.org/10.1007/s10404-006-0141-4

[3] M. R. Safaei, H. Togun, K. Vafai, S. N. Kazi, and A. Badarudin, "Investigation of Heat Transfer Enhancement in a Forward-Facing Contracting Channel Using FMWCNT Nanofluids," *Numerical Heat Transfer, Part A: Applications*, vol. 66, no. 12, pp. 1321–1340, 2014. [Online]. Available: https://doi.org/10.1080/10407782.2014.916101

[4] A. Karimipour, M. Hemmat Esfe, M. R. Safaei, D. Toghraie Semiromi, S. Jafari, and S. N. Kazi, "Mixed convection of copper–water nanofluid in a shallow inclined lid driven cavity using the lattice Boltzmann method," *Physica A: Statistical Mechanics and its Applications*, vol. 402, pp. 150–168, 2014. [Online]. Available: https://doi.org/10.1016/j.physa.2014.01.057

[5] J.-Y. Jung, H.-S. Oh, and H.-Y. Kwak, "Forced convective heat transfer of nanofluids in microchannels," *International Journal of Heat and Mass Transfer*, vol. 52, no. 1–2, pp. 466–472, 2009. [Online]. Available: https://doi.org/10.1016/j.ijheatmasstransfer.2008.03.033

[6] C. J. Ho, L. C. Wei, and Z. W. Li, "An experimental investigation of forced convective cooling performance of a microchannel heat sink with Al2O3/water nanofluid," *Applied Thermal Engineering*, vol. 30, no. 2–3, pp. 96–103, 2010. [Online]. Available: https://doi.org/10.1016/j.applthermaleng.2009.07.003

[7] Y. Zhou, R. Zhang, I. Staroselsky, H. Chen, W. T. Kim, and M. S. Jhon, "Simulation of micro- and nano-scale flows via the lattice Boltzmann method," *Physica A: Statistical Mechanics and its Applications*, vol. 362, no. 1, pp. 68–77, 2006. [Online]. Available: https://doi.org/10.1016/j.physa.2005.09.037

[8] S. Succi, "Mesoscopic Modeling of Slip Motion at Fluid-Solid Interfaces with Heterogeneous Catalysis," *Physical Review Letters*, vol. 89, no. 6, p. 064502, 2002. [Online]. Available: https://doi.org/10.1103/PhysRevLett.89.064502

[9] Y.-T. Yang and F.-H. Lai, "Lattice Boltzmann simulation of heat transfer and fluid flow in a microchannel with nanofluids," *Heat and Mass Transfer*, vol. 47, no. 10, pp. 1229–1240, 2011. [Online]. Available: https://doi.org/10.1007/s00231-011-0786-8

[10] D. C. Tretheway and C. D. Meinhart, "Apparent fluid slip at hydrophobic microchannel walls," *Physics of Fluids*, vol. 14, no. 3, pp. L9–L12, 2002. [Online]. Available: https://doi.org/10.1063/1.1432696

[11] A. Raisi, B. Ghasemi, and S. M. Aminossadati, "A Numerical Study on the Forced Convection of Laminar Nanofluid in a Microchannel with Both Slip and No-Slip Conditions," *Numerical Heat Transfer, Part A: Applications*, vol. 59, no. 2, pp. 114–129, 2011. [Online]. Available: https://doi.org/10.1080/10407782.2011.540964

[12] Z. Nikkhah, A. Karimipour, M. R. Safaei, P. Forghani-Tehrani, M. Goodarzi, M. Dahari, and S. Wongwises, "Forced convective heat transfer of water/functionalized multi-walled carbon nanotube nanofluids in a microchannel with oscillating heat flux and slip boundary condition," *International Communications in Heat and Mass Transfer*, vol. 68, pp. 69–77, 2015. [Online]. Available: https://doi.org/10.1016/j.icheatmasstransfer.2015.08.008

[13] C. Cercignani and A. Daneri, "Flow of a Rarefied Gas between Two Parallel Plates," *Journal of Applied Physics*, vol. 34, no. 12, pp. 3509–3513, 1963. [Online]. Available: https://doi.org/10.1063/1.1729249

[14] A. D'Orazio, Z. Nikkhah, and A. Karimipour, "Simulation of copper–water nanofluid in a microchannel in slip flow regime using the lattice Boltzmann method with heat flux boundary condition," *Journal of Physics: Conference Series*, vol. 655, p. 012029, 2015. [Online]. Available: https://doi.org/10.1088/1742-6596/655/1/012029

[15] A. Karimipour, A. Hossein Nezhad, A. D'Orazio, M. Hemmat Esfe, M. R. Safaei, and E. Shirani, "Simulation of copper–water nanofluid in a microchannel in slip flow regime using the lattice Boltzmann method," *European Journal of Mechanics - B/Fluids*, vol. 49, pp. 89–99, 2015. [Online]. Available: https://doi.org/10.1016/j.euromechflu.2014.08.004

[16] G. P. Celata, L. M. Cumo, M. McPhail, and G. Zummo, "Characterization of fluid dynamic behaviour and channel wall effects in microtube," *International Journal of Heat and Fluid Flow*, vol. 27, no. 1, pp. 135–143, 2006. [Online]. Available: https://doi.org/10.1016/j.ijheatfluidflow.2005.03.012

[17] W. Qu, S.-Y. Lee, S. T. Wereley, and I. Mudawar, "Experimental and Computational Investigation of

Flow Development and Pressure Drop in a Rectangular Micro-channel," *Journal of Electronic Packaging*, vol. 128, no. 1, pp. 1–9, 2006. [Online]. Available: https://doi.org/10.1115/1.2159002

[18] M. Abbaszadeh, A. Ababaei, A. A. Arani, and A. A. Sharifabadi, "MHD forced convection and entropy generation of CuO-water nanofluid in a microchannel considering slip velocity and temperature jump," *Journal of the Brazilian Society of Mechanical Sciences and Engineering*, vol. 39, no. 3, pp. 775–790, 2017. [Online]. Available: https://doi.org/10.1007/s40430-016-0578-7

[19] S. Noreen, S. Waheed, and A. Hussanan, "Peristaltic motion of MHD nanofluid in an asymmetric micro-channel with Joule heating, wall flexibility and different zeta potential," *Boundary Value Problems*, vol. 2019, no. 1, p. 12, 2019. [Online]. Available: https://doi.org/10.1186/s13661-019-1118-z

[20] A. López, G. Ibáñez, J. Pantoja, J. Moreira, and O. Lastres, "Entropy generation analysis of MHD nanofluid flow in a porous vertical microchannel with nonlinear thermal radiation, slip flow and convective-radiative boundary conditions," *International Journal of Heat and Mass Transfer*, vol. 107, pp. 982–994, 2017. [Online]. Available: https://doi.org/10.1016/j.ijheatmasstransfer.2016.10.126

[21] A. Akbarinia, M. Abdolzadeh, and R. Laur, "Critical investigation of heat transfer enhancement using nanofluids in microchannels with slip and non-slip flow regimes," *Applied Thermal Engineering*, vol. 31, no. 4, pp. 556–565, 2011. [Online]. Available: https://doi.org/10.1016/j.applthermaleng.2010.10.017

[22] A. A. A. A. Al-Rashed, A. Shahsavar, O. Rasooli, M. A. Moghimi, A. Karimipour, and M. D. Tran, "Numerical assessment into the hydrothermal and entropy generation characteristics of biological water-silver nano-fluid in a wavy walled microchannel heat sink," *International Communications in Heat and Mass Transfer*, vol. 104, pp. 118–126, 2019. [Online]. Available: https://doi.org/10.1016/j.icheatmasstransfer.2019.03.007

[23] S. E. Ghasemi, A. A. Ranjbar, and M. J. Hosseini, "Thermal and hydrodynamic characteristics of water-based suspensions of Al2O3 nanoparticles in a novel minichannel heat sink," *Journal of Molecular Liquids*, vol. 230, pp. 550–556, 2017. [Online]. Available: https://doi.org/10.1016/j.molliq.2017.01.066

[24] L. Goldstein, Jr. and E. M. Sparrow, "Heat/Mass Transfer Characteristics for Flow in a Corrugated Wall Channel," *Journal of Heat Transfer*, vol. 99, no. 2, pp. 187–195, 1977. [Online]. Available: https://doi.org/10.1115/1.3450667

[25] Y. Sui, P. S. Lee, and C. J. Teo, "An experimental study of flow friction and heat transfer in wavy microchannels with rectangular cross section," *International Journal of Thermal Sciences*, vol. 50, no. 12, pp. 2473–2482, 2011. [Online]. Available: https://doi.org/10.1016/j.ijthermalsci.2011.06.017

[26] M. M. Sarafraz and F. Hormozi, "Intensification of forced convection heat transfer using biological nanofluid in a double-pipe heat exchanger," *Experimental Thermal and Fluid Science*, vol. 66, pp. 279–289, 2015. [Online]. Available: https://doi.org/10.1016/j.expthermflusci.2015.03.028

[27] W. A. Ebert and E. M. Sparrow, "Slip Flow in Rectangular and Annular Ducts," *Journal of Basic Engineering*, vol. 87, no. 4, pp. 1018–1024, 1965. [Online]. Available: https://doi.org/10.1115/1.3650793

[28] K. Anoop and R. Sadr, "Measurement of Optical Properties of Nanofluids and its Effects in Near-wall Flow Evaluation," in Proceeding 7th International Conference on Quantum, Nano and Micro Technologies, pp. 82–87. 2013.